

Parkin regulates mitophagy and mitochondrial function to protect against alcohol-induced liver injury and steatosis in mice

Jessica A. Williams, Hong-Min Ni, Yifeng Ding, and Wen-Xing Ding

Department of Pharmacology, Toxicology and Therapeutics, University of Kansas Medical Center, Kansas City, Kansas

Submitted 13 April 2015; accepted in final form 27 June 2015

Williams JA, Ni HM, Ding Y, Ding WX. Parkin regulates mitophagy and mitochondrial function to protect against alcohol-induced liver injury and steatosis in mice. *Am J Physiol Gastrointest Liver Physiol* 309: G324–G340, 2015. First published July 9, 2015; doi:10.1152/ajpgi.00108.2015.—Alcoholic liver disease claims two million lives per year. We previously reported that autophagy protected against alcohol-induced liver injury and steatosis by removing damaged mitochondria. However, the mechanisms for removal of these mitochondria are unknown. Parkin is an evolutionarily conserved E3 ligase that is recruited to damaged mitochondria to initiate ubiquitination of mitochondrial outer membrane proteins and subsequent mitochondrial degradation by mitophagy. In addition to its role in mitophagy, Parkin has been shown to have other roles in maintaining mitochondrial function. We investigated whether Parkin protected against alcohol-induced liver injury and steatosis using wild-type (WT) and Parkin knockout (KO) mice treated with alcohol by the acute-binge and Gao-binge (chronic plus acute-binge) models. We found that Parkin protected against liver injury in both alcohol models, likely because of Parkin's role in maintaining a population of healthy mitochondria. Alcohol caused greater mitochondrial damage and oxidative stress in Parkin KO livers compared with WT livers. After alcohol treatment, Parkin KO mice had severely swollen and damaged mitochondria that lacked cristae, which were not seen in WT mice. Furthermore, Parkin KO mice had decreased mitophagy, β -oxidation, mitochondrial respiration, and cytochrome *c* oxidase activity after acute alcohol treatment compared with WT mice. Interestingly, liver mitochondria seemed able to adapt to alcohol treatment, but Parkin KO mouse liver mitochondria had less capacity to adapt to Gao-binge treatment compared with WT mouse liver mitochondria. Overall, our findings indicate that Parkin is an important mediator of protection against alcohol-induced mitochondrial damage, steatosis, and liver injury.

autophagy; mitophagy; Parkin; alcohol; steatosis; liver injury

ALCOHOLIC LIVER DISEASE (ALD) is a health problem worldwide that claims two million lives per year (36), and 50% of people in the United States over the age of 18 consume alcohol regularly (28). ALD pathogenesis begins with liver steatosis, which is reversible with abstinence from alcohol. However, with continuous alcohol abuse, ALD can progress in some patients from steatosis to steatohepatitis, fibrosis, cirrhosis, and even hepatocellular carcinoma with prolonged alcohol abuse. Mechanisms for progression of ALD pathogenesis are still not completely understood. In addition, there is currently no cure for ALD other than liver transplantation in severe disease states (5, 13, 45). Therefore, a better understanding of mechanisms involved in ALD pathogenesis is greatly needed for future

generation of therapeutics to combat liver disease caused by alcohol.

Macroautophagy (hereafter referred to as autophagy) is a protective process that initiates lysosomal degradation of cellular components. Autophagy is activated to provide the cell with nutrients during starvation or to remove damaged organelles and protein aggregates to prevent cell death and tissue injury. Autophagy occurs through formation of double-membrane autophagosomes, which engulf organelles and protein aggregates and shuttle them to the lysosome for degradation (34). We and others have previously shown that autophagy is protective against alcohol-induced liver injury (9, 10, 21). Specifically, we found that autophagy protected against alcohol-induced liver injury and steatosis by selectively removing damaged mitochondria and lipid droplets by mitophagy and lipophagy, respectively (9, 10). Mitophagy has been shown to be activated as a protective mechanism by many different cellular stress conditions including loss of mitochondrial membrane potential, cellular reactive oxygen species (ROS) accumulation, mitochondrial DNA damage, and mitochondrial accumulation of aggregated proteins (23). Some of these stresses, such as cellular ROS and nitric oxide accumulation and mitochondrial DNA damage, have been associated with ALD pathogenesis (1, 14, 49) and likely lead to alcohol-induced mitophagy activation in the liver (18). However, mechanisms for alcohol-induced activation of mitophagy in the liver are currently unknown.

Mitophagy has been shown to require Parkin in *in vitro* models (6–8, 27). Parkin is an evolutionarily conserved E3 ligase that is recruited to damaged mitochondria by phosphatase and tensin homolog-induced putative kinase 1 (Pink1) to initiate ubiquitination of mitochondrial outer membrane proteins and subsequent mitochondrial degradation by mitophagy (6, 7, 17, 26, 27). Parkin is mainly known for its protective role in the brain because loss of Parkin has been linked to autosomal recessive Parkinsonism (19), but we found that Parkin is also expressed in liver (12). The role of Parkin-induced mitophagy *in vivo* is not completely understood. We recently demonstrated that Parkin translocated to liver mitochondria after acetaminophen treatment in mice. In addition, mitophagy levels were decreased in Parkin knockout (KO) mice compared with wild-type (WT) mice after acetaminophen treatment, suggesting that removal of damaged mitochondria by Parkin-induced mitophagy is likely a protective mechanism in the liver (46). In addition to its role in mitophagy, Parkin has also been shown to help maintain mitochondrial function in the brain. Parkin KO mouse brain mitochondria had decreased mitochondrial respiration and dysregulation of proteins involved in energy metabolism and respiration with aging (33, 35, 42). Therefore, we investigated the role of Parkin in mitophagy induction and in maintenance of mitochondrial function as

Address for reprint requests and other correspondence: W.-X. Ding, Dept. of Pharmacology, Toxicology and Therapeutics, Univ. of Kansas Medical Center, MS 1018, 3901 Rainbow Blvd., Kansas City, KS 66160 (e-mail: wxding@KUMC.edu).

protective mechanisms against alcohol-induced liver injury using WT and Parkin KO mice. Two mouse alcohol models were used in this study: acute-binge and Gao-binge (chronic plus acute-binge). The acute-binge model represents human binge drinking, which is defined as consumption of greater than 4 or 5 drinks in a 2-h period for women and men, respectively (39). The acute-binge model is best for studying initial phases of ALD because it causes slight liver injury, steatosis, oxidative stress, and mitochondrial damage and dysfunction (25, 39). The Gao-binge model is thought to better reflect human disease because most chronic alcohol abusers also binge drink, and binge drinking in chronic alcohol abusers is thought to further progression from alcohol-induced steatosis to more severe liver pathologies, such as steatohepatitis. In addition, the Gao-binge alcohol model produces greater amounts of liver injury and steatosis than the acute-binge model while also producing mitochondrial damage and oxidative stress (3, 4, 25, 29, 45).

We found that Parkin KO mice had increased liver injury, oxidative stress, and steatosis after alcohol treatment compared with WT mice. Parkin KO mouse livers had decreased mitophagy, β -oxidation, mitochondrial respiration, and cytochrome *c* oxidase (COX) activity compared with WT mouse livers after acute-binge alcohol treatment. Decreased hepatic mitochondrial function in Parkin KO mice was likely due to increased alcohol-induced mitochondrial damage and reduced mitophagy compared with WT mice. Interestingly, liver mitochondria seemed able to adapt to Gao-binge treatment, but mitochondria from Parkin KO mouse livers seemed less able to adapt to alcohol compared with WT mouse mitochondria, resulting in severely damaged and swollen mitochondria in Parkin KO mouse livers. Our findings indicate that Parkin is an important protector against alcohol-induced liver injury and steatosis owing to its roles in maintaining mitochondrial integrity and function after alcohol treatment.

MATERIALS AND METHODS

Materials. Two hundred proof ethanol (DSP-MD.43), maltose dextran (3653), and the Lieber-DeCarli '82 Shake and Pour Liquid Control (F1259SP) and Ethanol (F1258SP) diets were all purchased from Bio-Serv. The kit used for alanine aminotransferase (ALT) measurement was purchased from Pointe Scientific (A7526-450). The following antibodies were used for Western blot analysis: anti-Cyp2e1 (Abcam, ab19140), anti- β -Actin (Sigma, A5441), anti-Fasn (Cell Signaling, 3180S), anti-Acc (Cell Signaling, 3676S), anti-Parkin (Santa-Cruz, SC-32282), anti-GAPDH (Cell Signaling, 2118), anti-Tom20 (Santa-Cruz, SC11415), anti-p62 (Abnova, H00008878-M01), anti-HSP60 (Santa Cruz, sc-13115), anti-VDAC (Calbiochem, 529534), and anti-Cox II (Mitoscience, D1203). The anti-LC3 antibody was generated as previously described (9).

Animal experiments. WT C57BL/6J and whole body Parkin KO mice (C57BL/6J background, no. 006582) were purchased from the Jackson Laboratory. All animals received humane treatment, and all protocols were approved by the Institutional Animal Care and Use Committee at the University of Kansas Medical Center. Eight- to 12-wk-old male mice were treated with ethanol by one of two models: acute-binge (9) or Gao-binge (3, 45). For acute binge, mice were fasted for 6 h in the morning and then given ethanol (4.5 g/kg body wt) or an equivalent volume of water by oral gavage, which was spaced over four gavages spread 15 min apart. Mice were euthanized 16 h after binge. For Gao-binge, mice were acclimated to the Lieber-DeCarli liquid control diet for 5 days followed by further feeding with the liquid control or ethanol diet for 10 days. The mice were then

given an 8-h ethanol (5 g/kg body wt) or maltose dextran (9 g/kg body wt) binge by oral gavage on the morning of *day 16* (*day 11* after the start of alcohol diet feeding). Gavages for Gao-binge were spaced over two gavages spread 15 min apart. The volume of control diet given to mice was matched to the volume of ethanol diet consumed. Liver injury was determined by measuring serum ALT.

Western blot analysis. Total liver lysates were prepared by using radioimmunoprecipitation assay (RIPA) buffer [1% Nonidet P-40, 0.5% sodium deoxycholate, 0.1% sodium dodecyl (lauryl) sulfate]. Heavy membrane (HM) enriched with mitochondria and cytosolic fractions were prepared as described previously (11). Briefly, liver tissues were homogenized in HIM buffer [200 mM mannitol, 70 mM sucrose, 5 mM HEPES, 0.5 mM EGTA (pH 7.5)] containing protease inhibitors by use of a Dounce homogenizer. Homogenates were centrifuged at 1,000 g to remove debris and nuclei, and the supernatant was centrifuged at 10,000 g for 10 min to separate HM and cytosolic fractions. The supernatant was kept as the cytosolic fraction, and the pellet containing the HM fraction was further washed by centrifugation and resuspended in HIM buffer. Protein (20–30 μ g) was separated by a 12% SDS-PAGE gel before transfer to a PVDF membrane. Membranes were probed with appropriate primary and secondary antibodies and developed with SuperSignal West Pico chemiluminescent substrate (Life Technologies, 34080).

RNA isolation and real-time qPCR. RNA was isolated from mouse livers by use of TRIzol reagent (Ambion, 15596-026) and was reverse-transcribed into cDNA with RevertAid Reverse Transcriptase (Fermentas, EP0442). Quantitative PCR (qPCR) was performed by use of SYBR Green chemistry (Bio-Rad, 1725124). Primer sequences (5'–3') for primers used in qPCR are Acca forward (F): CTCCAG-GACAGCACAGATCA, reverse (R): TGACTGCCGAAACA-TCTCTG; Fasn F: TGGGTTCTAGCCAGCAGAGT, R: ACCACCA-GAGACCGTTATGC; Srebp1 F: GATCAAAGAGGAGCCAGTGC, R: TAGATGGTGGCTGCTGAGTG; Acox1 F: CAGGAAGAG-CAAGGAAGTGG, R: CCTTTCTGGCTGATCCCAT; Cpt1 α F: CCAGGTACAGTGGGACATT, R: GAACCTGGCCATGTCCT-TGT; Ppara F: ATGCCAGTACTGCCGTTTTC, R: GGCCTTGACCT-TGTTTCATGT; β -actin F: TGTTACCAACTGGGACGACA, R: GGGGTGTTGAAGGTCTCAAA. Real-time qPCR results were normalized to β -actin and expressed as fold over WT control (water binge or control diet, where appropriate).

Histology. For hematoxylin and eosin (H&E) staining, formalin-fixed liver sections were embedded in paraffin and cut into 5- μ m sections before staining with H&E. For 4-hydroxynonenal (4HNE) staining, 5- μ m paraffin sections were incubated with 4HNE antibody (Alpha Diagnostics, HNE11-S, 1:250) by a standard immunohistochemistry procedure. Briefly, tissue sections were incubated with primary antibody for 30 min after deparaffinization and antigen retrieval in citrate buffer. Sections were then washed and incubated with signal stain boost (Cell Signaling, 8114S) for 30 min and developed by use of diaminobenzidine substrate (Vector, SK4105). Tissues were counterstained with hematoxylin. Positive areas were determined by Image J and calculated as a percentage of liver area. For Oil Red O staining, tissues were fixed in 4% paraformaldehyde overnight at 4°C and then transferred to 20% sucrose and stored at 4°C for ~24 h before mounting in OCT compound and freezing at –20°C; 6 μ m sections were used for staining. Briefly, tissues were washed twice with PBS and then incubated with 60% isopropanol for 1 min. Tissues were dried in a 37°C incubator for ~10 min before incubating with Oil Red O solution. Oil Red O solution was prepared by adding 0.35 g Oil Red O (Sigma, 0625) to 100 ml of 100% isopropanol, which was further diluted 1.7 times in water and filtered immediately before use. Slides were incubated with Oil Red O solution for 15 min. The Oil Red O solution was aspirated from the slides, and 60% isopropanol was added to the slides for several min to remove any residual Oil Red O. Slides were then washed in PBS and stained for 30 s with hematoxylin (Sigma, GHS132) followed by more washes in dH₂O. Slides were mounted with glycerol (5:1 in PBS).

Measurement of liver triglycerides. Approximately 20–50 mg of liver tissue was ground into powder in liquid nitrogen with a mortar and pestle. Triglycerides were extracted by incubating the powdered tissue in a chloroform-methanol mix (2:1) for 1 h with vigorous shaking, 200 μ l of water was added to the samples, and the samples were vortexed and centrifuged at 3,000 g for 5 min to separate out the lipid phase. The lipid phase was removed and dried, and the remaining pellet containing lipids was dissolved in a *tert*-butanol and Triton X-114-methanol (2:1) mixture. Triglyceride levels were measured by colorimetric assay with a kit from Pointe Scientific (T7532-500).

Electron microscopy. Tissues were fixed with 2% glutaraldehyde in 0.1 M phosphate buffer (pH 7.4) followed by 1% OsO₄. After dehydration, thin sections were stained with uranyl acetate and lead citrate for observation under a JEM 1016CX electron microscope.

Mitochondrial respiration. Complex I (glutamate/malate) mitochondrial respiration was measured by the Oroboros instrument. Mouse liver mitochondria were freshly isolated after acute-binge ethanol treatment and stored on ice until use. To isolate mitochondria, mouse liver tissue was minced in 10 ml of mitochondria isolation buffer (70 mM sucrose, 210 mM mannitol, 5 mM HEPES, 1 mM EDTA) with 0.5% BSA by using four strokes of a Dounce homogenizer. The samples were then centrifuged at 800 g for 10 min to remove debris and nuclei, and the supernatant was decanted through cheesecloth before being centrifuged at 8,000 g for 10 min. The pellet containing mitochondria was resuspended in 100 μ l of mitochondria isolation buffer and washed by centrifugation at 8,000 g before final resuspension in 50 μ l of mitochondria isolation buffer. Mitochondrial respiration was assessed using 500 μ g of protein. We measured state 3, or ADP-dependent, respiration by adding the substrates glutamate (5 μ M) and malate (5 μ M) along with a limiting amount of ADP (0.45 μ M) to isolated liver mitochondria after acute-binge treatment. State 3 respiration represents respiration that is coupled to ATP synthesis because substrate is present along with ADP. We measured state 4, or ADP-independent, respiration by adding oligomycin (1 μ M) to totally deplete ADP levels after measurement of state 3 respiration. State 4 respiration represents respiration that is not coupled to ATP synthesis because substrate is present, but ADP is not. Carbonyl cyanide 4-(trifluoromethoxy) phenylhydrazone (FCCP, 0.1 μ M) was then added to uncouple mitochondria to measure maximal respiratory capacity. Finally, the electron transport chain complex III and I inhibitors antimycin (2 μ M) and rotenone (5 μ M) were added to measure nonmitochondrial oxygen consumption of the sample. State 3 respiration was calculated by using the peak plateau after ADP addition. State 4 respiration was calculated by using the steady-state value after oligomycin addition. Maximal respiratory capacity was calculated by using the peak after FCCP addition. The steady-state value after antimycin and rotenone addition was subtracted from all values, and results were normalized to protein concentration, which was confirmed after completion of the respiration assay. Final results were normalized to individual controls for WT and Parkin KO mice.

COX activity. COX activity was measured by using mouse liver total protein lysates by a colorimetric assay from Sigma-Aldrich (CYTOCOX1) according to the manufacturer's instructions.

Statistical analysis. Statistical analysis was conducted with a one-way ANOVA analysis followed by a Holm-Sidak test or by a Student's *t*-test as indicated. A *P* < 0.05 was considered significant.

RESULTS

Parkin KO mice had increased liver injury after alcohol administration. WT and Parkin KO mice were treated with alcohol using two alcohol models: acute-binge and Gao-binge. Liver injury was determined by measuring serum ALT after alcohol treatment, and both WT and Parkin KO mice had increased liver injury after alcohol treatment compared with control treatments in both alcohol models. Parkin KO mice

also had increased liver injury compared with WT mice after both acute-binge and Gao-binge alcohol treatments, but the difference in injury between WT and Parkin KO mice was statistically significant only in the Gao-binge model. Basal ALT levels were similar between WT and Parkin KO mice in both alcohol models (Fig. 1, A and B). Liver injury was also overall higher in both WT and Parkin KO mice treated with alcohol in the Gao-binge model compared with mice treated with alcohol in the acute-binge model, as expected (4) (Fig. 1, A and B). Alcohol consumption is well known to induce cytochrome *P*-450 2e1 (Cyp2e1) expression, which can further cause oxidative stress in the liver (2, 20, 37). WT and Parkin KO mice both had marked inductions of Cyp2e1 after alcohol treatment with the Gao-binge model, but the changes of Cyp2e1 were mild with the acute-binge model. There were no differences in Cyp2e1 levels between WT and Parkin KO mouse livers, suggesting that increased liver injury in Parkin KO mice compared with WT mice was not due to elevated induction of Cyp2e1 (Fig. 1, C and D).

Parkin KO mice had increased steatosis compared with WT mice after acute-binge but not Gao-binge treatment. Treatment with alcohol using both the acute-binge and Gao-binge models caused liver steatosis in WT and Parkin KO mice, which was demonstrated by elevated liver triglycerides (Fig. 2, A and B) and increased visualization of lipid droplets by H&E staining (Fig. 2, C and D), Oil Red O staining (Fig. 2, E and F), and electron microscopy (EM; Fig. 2, G and H, and data not shown). The Gao-binge model produced more macrosteatosis compared with the acute-binge model in both WT and Parkin KO alcohol-treated mouse livers (Fig. 2, C–F). In addition, Parkin KO mice developed greater liver steatosis compared with WT mice after acute-binge alcohol treatment. Livers from acute-binge-treated Parkin KO mice had significantly increased triglyceride levels compared with acute-binge-treated WT mouse livers (Fig. 2A), which was confirmed by H&E and Oil Red O staining (Fig. 2, C and E). Acute-binge-treated Parkin KO mouse livers also had a significant increase in the number of lipid droplets per cell compared with acute-binge-treated WT mouse livers (Fig. 2, G and H). However, the Gao-binge model caused greater triglyceride accumulation in WT mouse livers compared with the acute-binge model, but triglyceride levels were similar between Parkin KO Gao-binge- and acute-binge-treated mouse livers (Fig. 2, A and B). Overall, these data suggest that acute-binge caused greater liver fat accumulation in Parkin KO mice compared with WT mice. In addition, the Gao-binge model caused greater steatosis in WT mouse livers compared with WT mouse livers treated with the acute-binge model, but the Gao-binge and acute-binge models both caused similar levels of steatosis in Parkin KO mouse livers.

Steatosis in WT and Parkin KO mouse alcohol-treated livers was not due to fatty acid synthesis. Alcohol has been shown to cause steatosis in the liver by elevating fatty acid synthesis in the intragastric infusion (16) and chronic alcohol feeding models (48). To determine whether increased liver steatosis after alcohol treatment in WT and Parkin KO mouse livers was due to increased fatty acid synthesis, expression levels of several fatty acid synthesis genes were measured in mouse livers after alcohol treatment using both the acute and Gao-binge models. Gene expression levels of the fatty acid synthesis enzymes acetyl-coA carboxylase (*Acc*) and fatty acid synthase (*Fasn*) did not significantly change after alcohol treat-

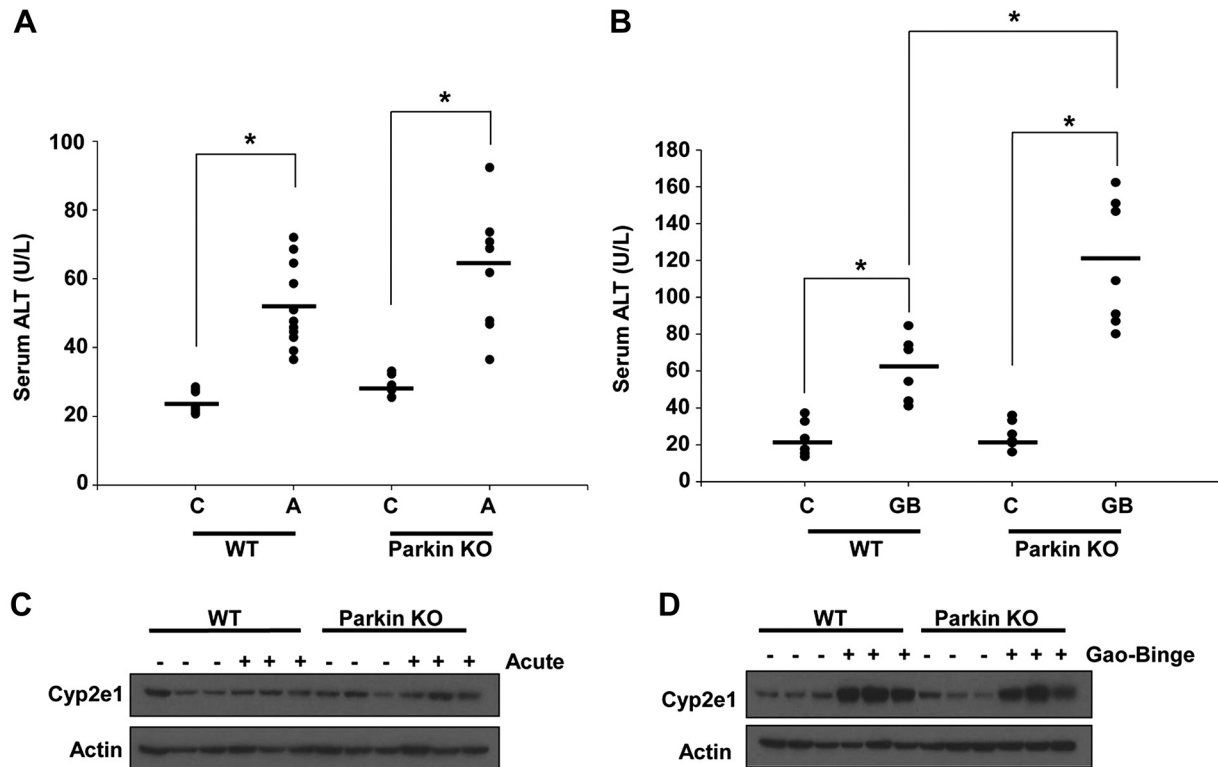


Fig. 1. Alcohol induced more liver injury in Parkin knockout (KO) mice. *A* and *B*: serum alanine aminotransferase (ALT) levels were measured from wild-type (WT) and Parkin KO mice after treatment with alcohol by using the acute-binge (*A*) or Gao-binge (*B*) model. Data shown are means \pm SE ($n \geq 5$ mice per group; $*P < 0.05$ by 1-way ANOVA). *C*, control; *A*, acute-binge; *GB*, Gao-binge. *C* and *D*: WT and Parkin KO mice were treated with the acute-binge (*C*) or Gao-binge (*D*) model, and liver lysates were analyzed by Western blot. β -Actin was used as a loading control.

ment by either the acute-binge or Gao-binge alcohol model in WT or Parkin KO mice compared with their individual controls. However, basal expression levels of these genes were decreased in Parkin KO mouse livers compared with WT mice in the acute model (Fig. 3, *A* and *B*). Liver gene expression levels for sterol regulatory element-binding transcription factor 1 (*Srebp1*) were significantly decreased in WT mouse ethanol-treated livers from both the acute and Gao-binge models compared with control livers. *Srebp1* gene expression was overall decreased in Parkin KO mouse livers compared with WT livers, but it was not significantly affected in Parkin KO mouse livers after alcohol treatment compared with Parkin KO control livers for either alcohol model (Fig. 3, *A* and *B*). Protein levels of Fasn and Acc were similar to mRNA levels (Fig. 3, *C* and *D*). These data suggest that alcohol-induced steatosis in WT and Parkin KO mouse livers was not likely due to an increase in fatty acid synthesis.

Greater steatosis in Parkin KO mouse livers after acute-binge alcohol treatment compared with WT mouse livers was due to decreased β -oxidation. Alcohol-induced inhibition of β -oxidation has been shown to cause fatty liver (41). To determine whether increased steatosis in WT and Parkin KO alcohol-treated mouse livers was due to decreased fat degradation by β -oxidation, expression levels of several genes involved in the β -oxidation pathway were measured including the enzymes peroxisomal acyl-coenzyme A oxidase 1 (*Acox1*) and carnitine palmitoyltransferase 1 alpha (*Cpt1a*) and the transcription factor peroxisome proliferator-activated receptor alpha (*Ppara*). In the acute-binge model, gene expression

levels for *Acox1* and *Ppara* were significantly increased after alcohol treatment in WT mouse livers compared with controls. However, there were no significant differences in expression of *Cpt1a* after acute-binge treatment in WT mouse livers compared with controls. Opposite to WT mice, expression levels of *Ppara* and *Acox1* in Parkin KO acute-binge-treated mouse livers did not increase compared with Parkin KO control-treated livers. Furthermore, the expression levels of *Acox1* and *Ppara* were significantly decreased in Parkin KO acute-binge-treated mouse livers compared with WT mouse livers. There was no significant change in the expression level of *Cpt1a* in acute-binge-treated Parkin KO mouse livers compared with acute-binge-treated WT mouse livers. There was no difference in basal expression levels for these genes between WT and Parkin KO mice (Fig. 3*E*). These data suggest that liver β -oxidation was likely activated as a protective mechanism in WT mouse livers after acute-binge alcohol treatment to help decrease liver steatosis. However, β -oxidation genes were not induced after acute-binge treatment in Parkin KO mouse livers, suggesting that liver β -oxidation may have been inhibited in Parkin KO mice treated with acute-binge. Decreased or inhibited β -oxidation in Parkin KO acute-binge-treated mouse livers may likely explain the greater levels of steatosis seen in Parkin KO acute-binge-treated mouse livers compared with WT acute-binge-treated livers (Fig. 2, *A*, *C*, *E*, *G*, and *H*).

Even though expression of β -oxidation genes was increased in WT mouse livers after acute ethanol treatment, expression of these genes was not induced by Gao-binge alcohol treatment in either WT or Parkin KO mouse livers compared with controls,

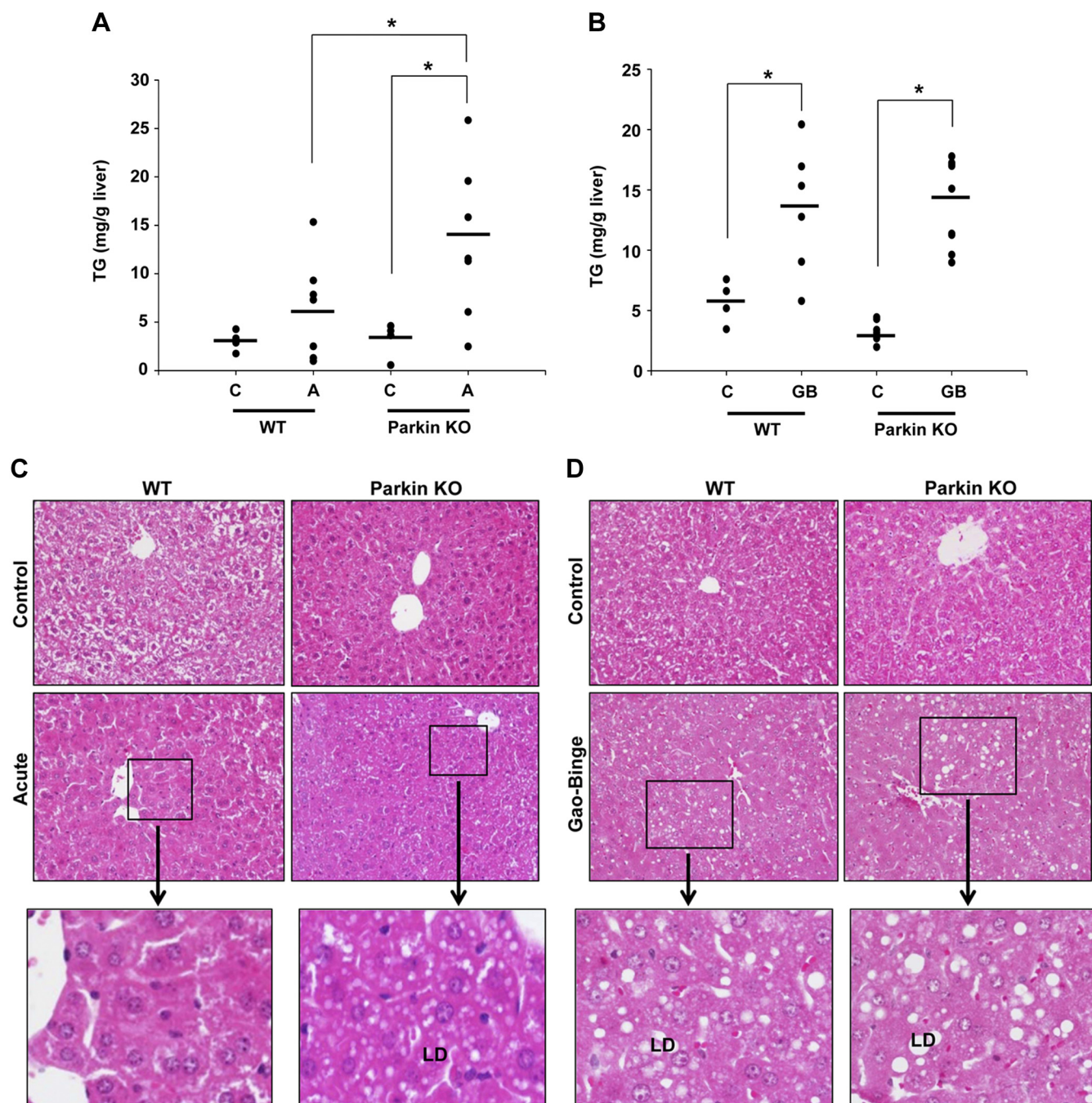


Fig. 2. Parkin KO mice had increased liver steatosis compared with WT mice after acute-binge, but not Gao-binge, treatment. *A* and *B*: liver triglycerides (TG) were measured for WT and Parkin KO mice after acute-binge (*A*) and Gao-binge (*B*) alcohol treatment. Data shown are means \pm SE ($n = 4$ for controls and ≥ 6 for alcohol-treated mice; $*P < 0.05$ by 1-way ANOVA). *C* and *D*: representative hematoxylin and eosin (H&E) images from the acute-binge model (*C*) and the Gao-binge model (*D*) are shown with boxed areas enlarged. LD, lipid droplet; $\times 200$ magnification. *E* and *F*: representative images are shown for Oil Red O staining for the acute-binge model (*E*) and for the Gao-binge model (*F*) with boxed areas enlarged ($\times 200$ magnification). *G*: representative electron microscopy (EM) images are shown for acute-binge-treated mice with boxed areas enlarged (bar = 500 nm; N, nucleus; M, mitochondria). *H*: quantification of lipid droplets per cell in acute-binge-treated mice. Data shown are means \pm SE ($n \geq 10$ images per mouse from 2 mice per group; $*P < 0.05$ by 1-way ANOVA).

suggesting that β -oxidation may have been inhibited in both WT and Parkin KO mouse livers after Gao-binge alcohol treatment. In fact, expression of β -oxidation genes was actually decreased in both WT and Parkin KO mouse livers after Gao-binge alcohol treatment compared with control-diet-fed mouse livers, but this decrease was only significant for *Cpt1a* gene expression in Parkin KO Gao-binge-treated livers. Sur-

prisingly, *Cpt1a* expression in Parkin KO mouse control-treated livers was significantly increased compared with WT control livers, suggesting that Parkin KO mice had higher levels of β -oxidation when fed the control diet compared with WT mice. There were no significant differences between Gao-binge-treated WT and Parkin KO mouse livers for any of the measured β -oxidation genes (Fig. 3*F*). Together, these data

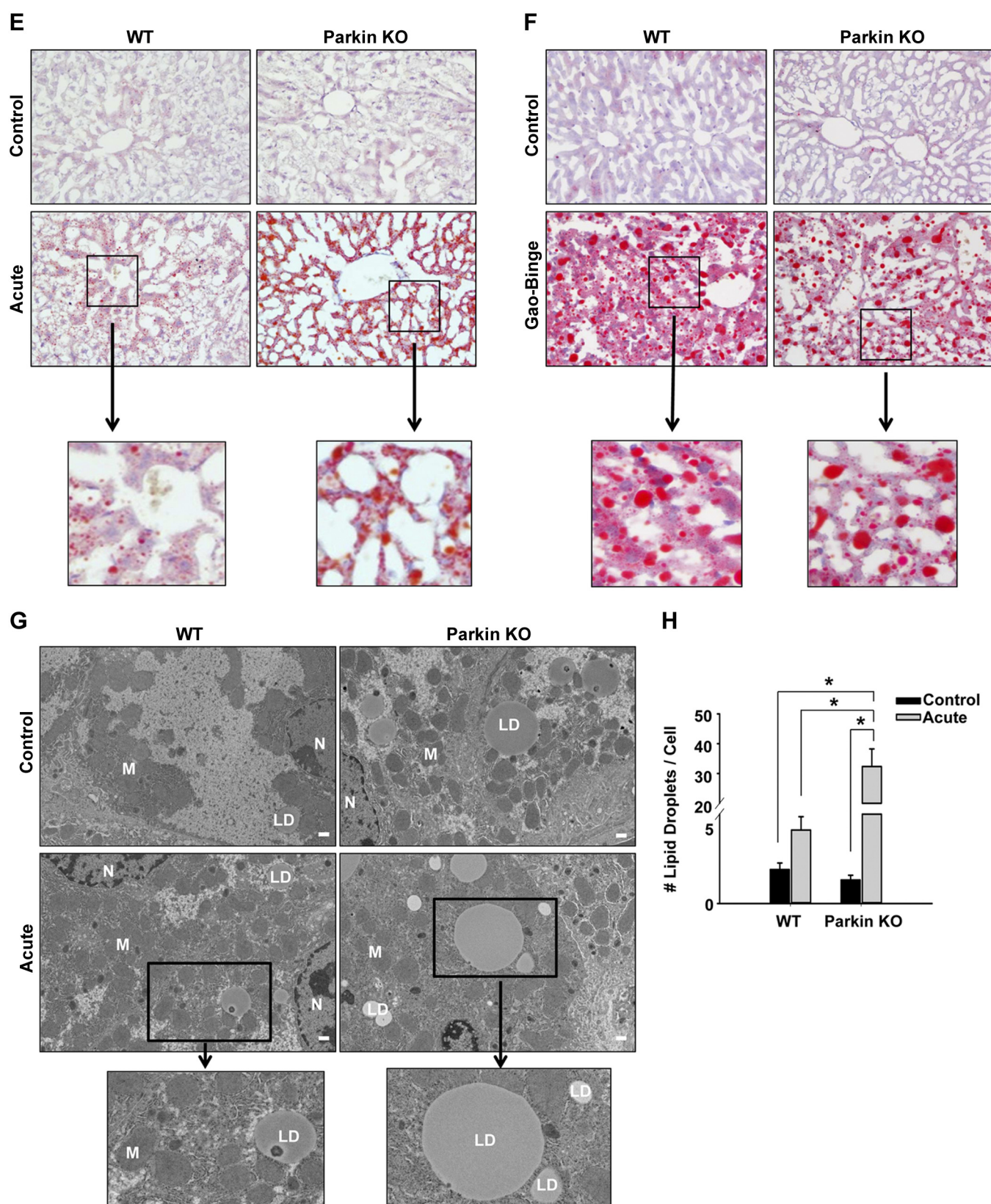


Fig. 2—Continued

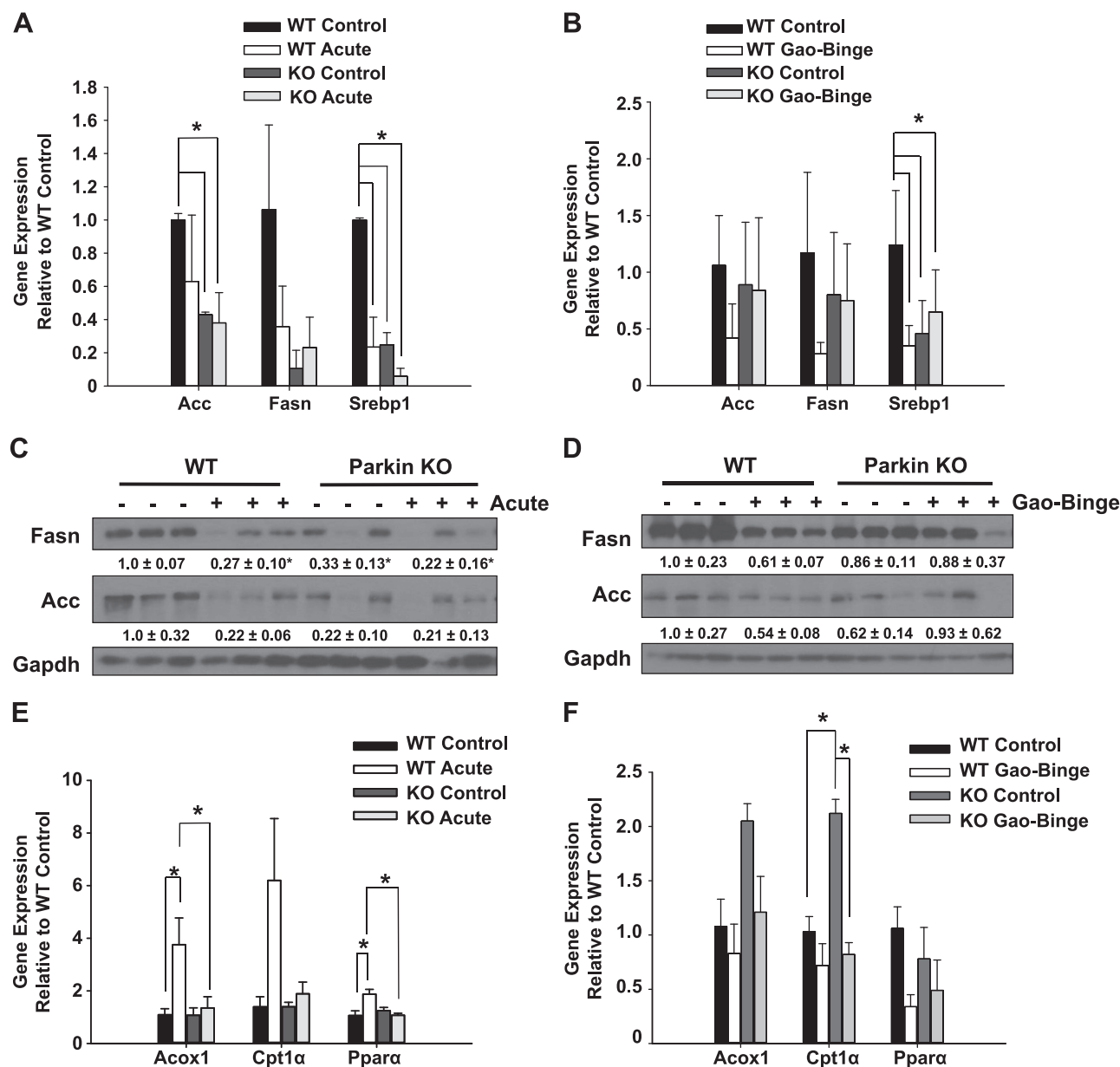


Fig. 3. Steatosis in WT and Parkin KO alcohol-treated livers was due not to fatty acid synthesis but to decreased β -oxidation. WT and Parkin KO mice were treated with the acute-binge (A, C and E) or Gao-binge (B, D and F) model. A, B, E and F: RNA from mouse livers was used to measure gene expression by quantitative PCR. Results were normalized to β -actin and expressed as fold change compared with WT control. Data shown are means \pm SD ($n = 3$ –4 mice per group; $*P < 0.05$ by 1-way ANOVA). C and D: protein was isolated from mouse livers for Western blot analysis. Results were normalized to Gapdh for densitometry analysis. Results from densitometry were expressed as fold change compared with WT control. Data shown are means \pm SE ($n = 3$ mice per group; $*P < 0.05$ by 1-way ANOVA).

suggest that β -oxidation was increased in acute-binge-treated WT mouse livers, which likely acted as an adaptive mechanism to reduce alcohol-induced liver steatosis. However, this protective adaptive mechanism seemed to be downregulated in Parkin KO acute-binge-treated mouse livers, which could be a reason for their increased alcohol-induced liver steatosis compared with WT mice. The protective response of β -oxidation seemed to be inhibited in both WT and Parkin KO mouse livers after Gao-binge alcohol treatment, which may explain why the levels of steatosis in WT and Parkin KO mouse livers were increased to similar levels after alcohol treatment using the Gao-binge model.

Reduced mitophagy in Parkin KO mice after alcohol treatment. Because decreased mitophagy could potentially lead to an increased population of damaged and dysfunctional mitochondria and subsequent liver injury, we compared levels of mitophagy between WT and Parkin KO mice after alcohol treatment using both the acute-binge and Gao-binge models. First, we determined whether Parkin translocated to mitochondria in WT mouse livers after alcohol treatment. Parkin did not translocate to mitochondria after acute-binge alcohol treatment for 3, 6, or 16 h (Fig. 4A and data not shown). However, Parkin did translocate to mitochondria after Gao-binge alcohol treatment in WT mouse livers (Fig. 4B), suggesting that Parkin-

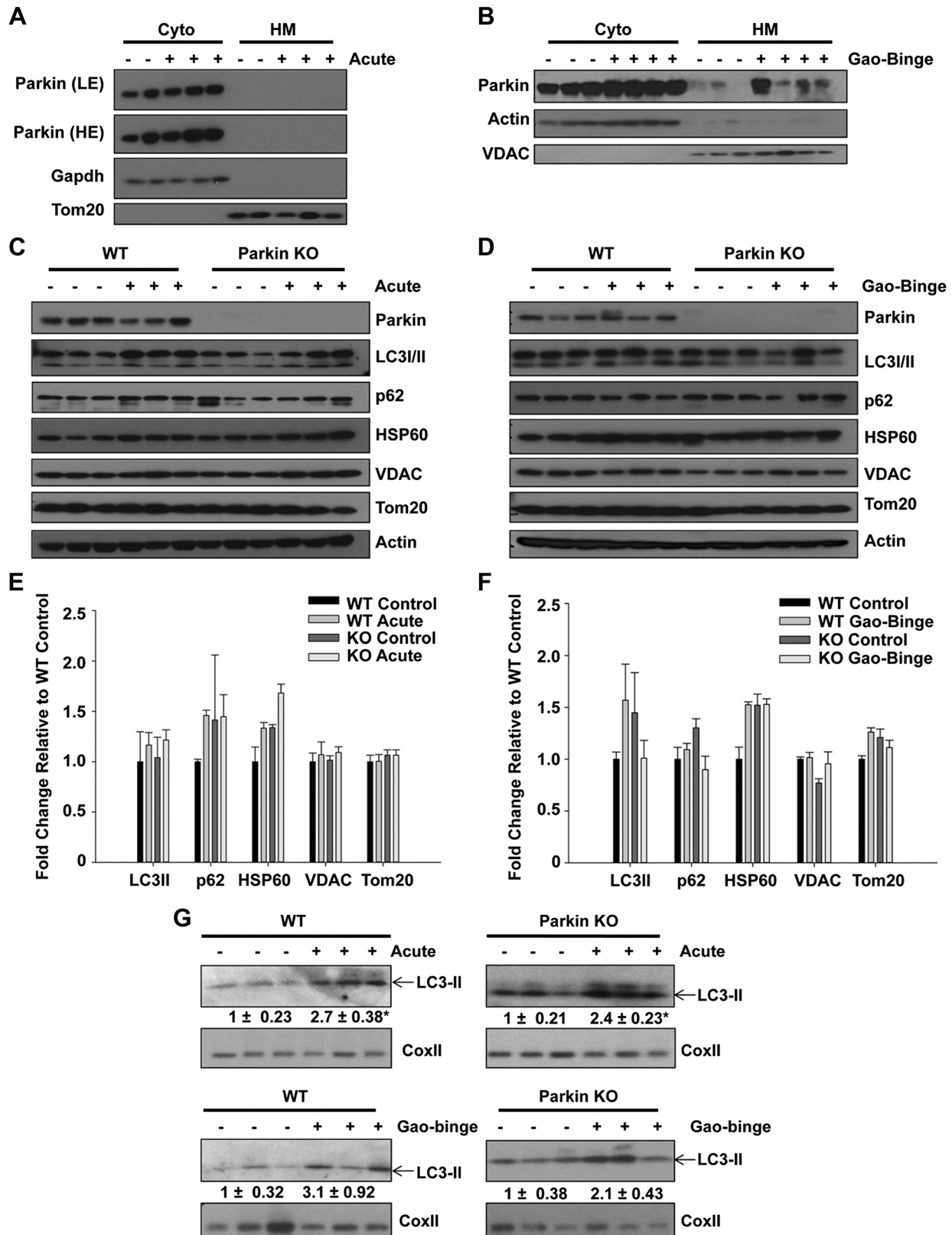
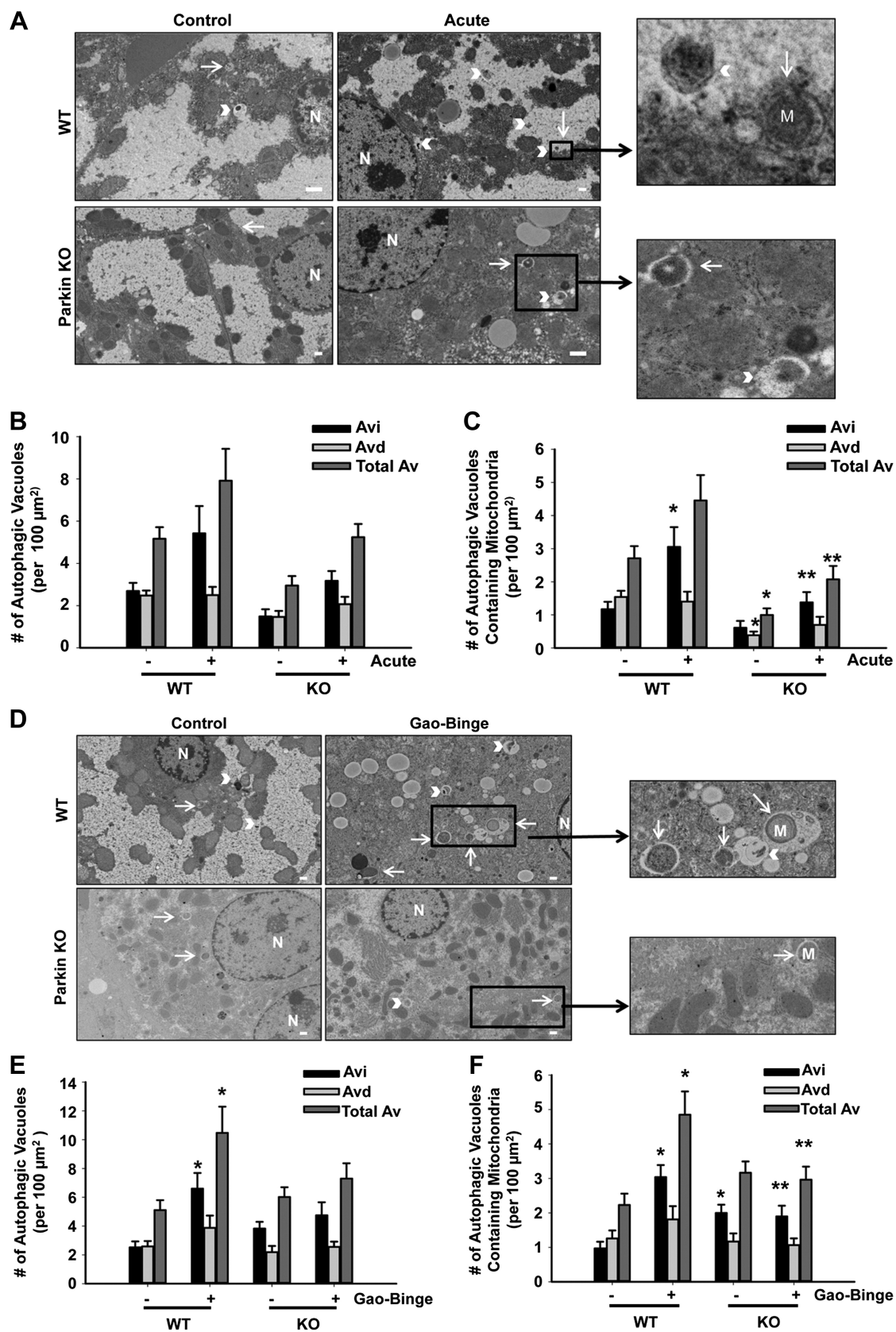


Fig. 4. Western blot analysis was unable to detect induction of mitophagy after alcohol treatment. *A* and *B*: WT and Parkin KO mice were treated with alcohol by using the acute-binge (*A*) and Gao-binge (*B*) models, and liver cytosolic (Cyto) and heavy membrane (HM) fractions were isolated and analyzed by Western blot. β -Actin or Gapdh and VDAC or Tom20 were used as loading controls. *C* and *D*: WT and Parkin KO mice were treated with alcohol by using the acute-binge (*C*) or Gao-binge (*D*) model, and liver lysates were used for Western blot analysis. β -Actin was used as a loading control. *E* and *F*: densitometry quantification for blots in *C* and *D*, respectively. Data shown are means \pm SE ($n = 3$ mice per group; no significant differences among groups by 1-way ANOVA). *G*: WT and Parkin KO mice were treated with alcohol by using the acute-binge or Gao-binge models, and HM fractions were used for Western blot analysis. Cox II was used as a loading control.



induced mitophagy may occur in WT mouse livers after Gao-binge alcohol treatment.

To further determine mitophagy levels between WT and Parkin KO mouse livers, we measured protein expression of the autophagy adaptor protein p62 and the autophagosome membrane protein microtubule-associated protein light chain 3 (LC3) in total liver lysates from WT and Parkin KO mice after acute-binge and Gao-binge treatment. There were no significant differences in p62 or LC3-II protein expression after alcohol treatment compared with controls in either alcohol model for WT or Parkin KO mice. In addition, there were no differences in expression of these proteins between WT and Parkin KO control mice (Fig. 4, C–F). There was also no degradation of the mitochondrial outer membrane proteins Translocase of outer membrane 20 (Tom20) or voltage-dependent anion channel (VDAC) or of the mitochondrial matrix protein heat shock protein 60 (Hsp60) after alcohol treatment by either the acute-binge or Gao-binge model in WT or Parkin KO mice (Fig. 4, C–F). These data suggest that mitophagy levels may be too mild to detect differences between WT and Parkin KO mice by Western blot analysis. Alternatively, mice may adapt to alcohol-induced mitochondrial damage by compensatory mitochondrial biogenesis, which can further offset mitophagic degradation determined by Western blot analysis. However, we observed increased levels of LC3-II protein in the heavy membrane fraction by Western blot after both acute-binge and Gao-binge alcohol treatments in WT and Parkin KO mouse livers (Fig. 4G), suggesting that there were increased autophagosome numbers induced by alcohol as we showed previously (9), and this increase was independent of Parkin.

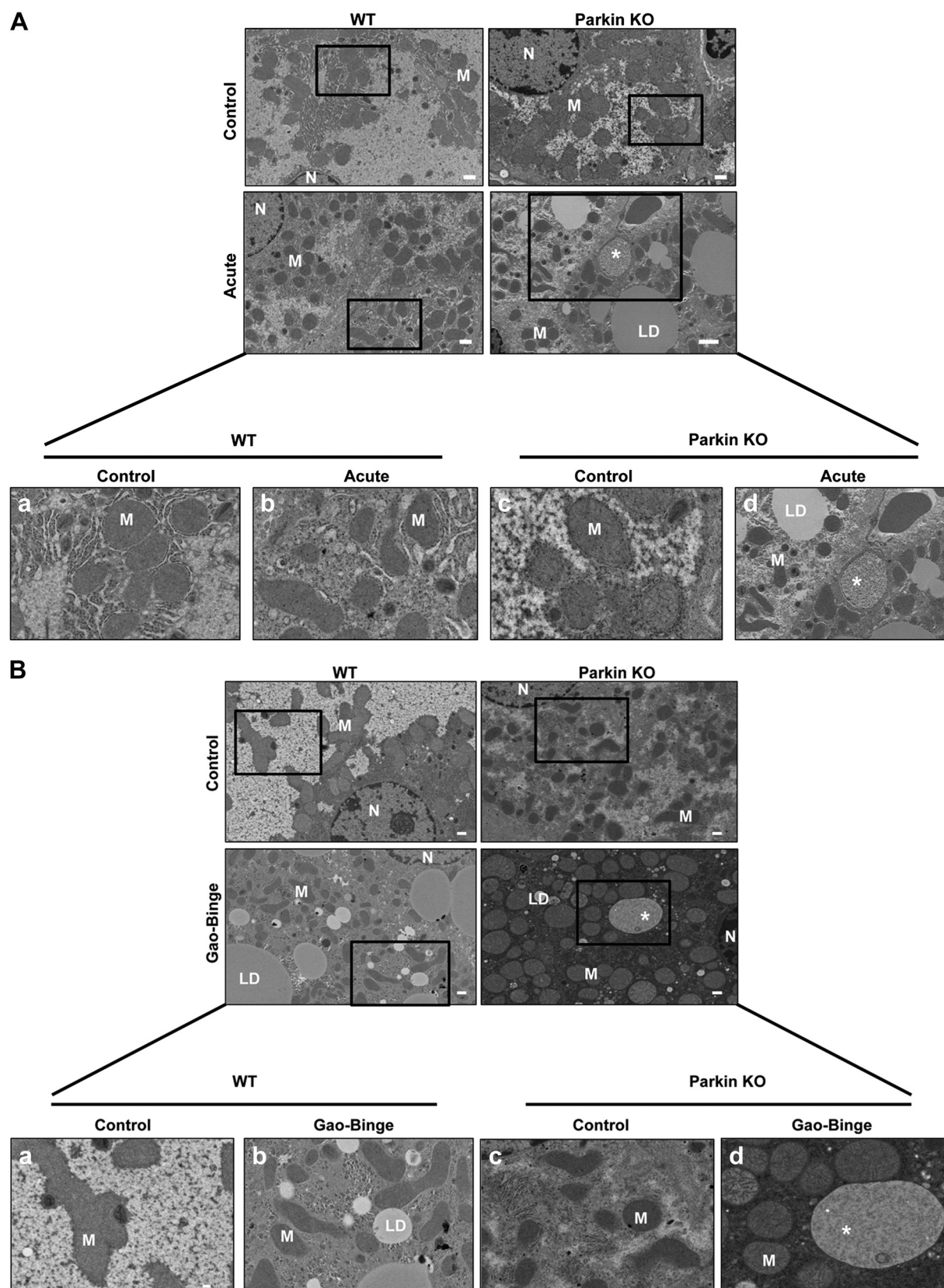
We next investigated whether there were differences in the number of autophagosomes and autolysosomes containing mitochondria (hereafter referred to as mitophagosomes) between WT and Parkin KO mouse livers after alcohol treatment using EM. In the acute-binge and Gao-binge alcohol models, the levels of mitophagy were significantly increased after alcohol treatment in WT mouse livers. However, the number of mitophagosomes was significantly decreased in Parkin KO mice compared with WT mice after alcohol treatment (Fig. 5, A, C, D, and F). The total number of autophagic vacuoles after alcohol treatment was also slightly decreased in Parkin KO mice compared with WT mice, but these data were not statistically significant (Fig. 5, A, B, D, and E). These data suggest that alcohol-induced mitophagy was decreased in Parkin KO mouse livers compared with WT mouse livers.

Mitochondrial morphological changes in the Gao-binge alcohol model. Chronic alcohol feeding has been shown to cause changes to mitochondrial morphology (15). Therefore, we determined whether alcohol treatment using the acute-binge or Gao-binge alcohol models caused changes to mitochondrial morphology in WT and Parkin KO mouse livers by EM.

Alcohol treatment by the acute-binge model did not cause any significant changes in mitochondrial morphology in WT mice compared with controls. However, some mitochondria in Parkin KO mouse livers appeared to have swelling after acute-binge treatment compared with control-treated liver mitochondria, but most mitochondria did not appear to be significantly damaged by alcohol treatment (Fig. 6A). Alcohol treatment using the Gao-binge model caused significantly damaged and swollen mitochondria in Parkin KO mouse livers where ~1% of mitochondria were so severely swollen and damaged that they lacked cristae. Only ~0.14% of mitochondria were this severely damaged in Parkin KO mice-treated with the acute-binge model (Fig. 6, B–D). These severely swollen and damaged mitochondria were not seen in WT mice after alcohol treatment with either model. In addition, Parkin KO mice had some liver mitochondria that were elongated after Gao-binge alcohol treatment, but WT mice appeared to have more elongated mitochondria after alcohol treatment by Gao-binge whereas Parkin KO mouse livers had more swollen mitochondria (Fig. 6F). Elongation of mitochondria is thought to be a cellular adaptive mechanism to chronic alcohol treatment (15). Acute-binge did not have a significant effect on mitochondrial elongation in either WT or Parkin KO mice (Fig. 6E). Overall, these results suggest that alcohol produced more damaged mitochondria in Parkin KO mouse livers compared with WT mouse livers, which may be due to an inability for Parkin KO mouse liver mitochondria to adapt to alcohol treatment or due to Parkin KO mouse livers having decreased mitophagy.

Mitochondrial respiration and COX activity were decreased in Parkin KO mice after alcohol treatment. To further determine whether Parkin KO mouse liver mitochondria were more damaged than WT mouse liver mitochondria after alcohol treatment, we investigated whether there were any differences in mitochondrial function between WT and Parkin KO mouse livers by measuring respiration rate and COX activity. We found that state 3 and state 4 respiration rates were both slightly increased in WT mouse liver mitochondria after acute-binge treatment compared with controls, but this increase was not statistically significant (Fig. 7, A and B). However, state 3 and state 4 respiration rates were decreased in Parkin KO mouse liver mitochondria after acute-binge treatment, which was statistically significant for state 3 respiration rates compared with acute-binge-treated WT mice (Fig. 7, A and B). Maximal respiratory capacity was also increased in WT mouse liver mitochondria after acute-binge treatment whereas it was decreased in Parkin KO mouse liver mitochondria (Fig. 7C). Basal respiration rates were similar between WT and Parkin KO mouse liver mitochondria (Fig. 7, A–C). COX activity was not affected by acute-binge treatment in WT mouse livers, but it was significantly decreased in Parkin KO mouse livers after acute-binge treatment compared with WT controls, suggesting that Parkin KO mouse liver mitochondria were more damaged

Fig. 5. Decreased mitophagy in Parkin KO mice. A: representative EM images are shown for the acute-binge model with boxed areas enlarged (arrows represent autophagosomes, and arrowheads represent autolysosomes; bar = 500 nm). B and C: quantification of the number of autophagic vacuoles (B) and mitophagosomes (C) from EM in A. Data shown are means \pm SE (n = 1 mouse per group, at least 15 images quantified per mouse; * P < 0.05 compared with WT control, ** P < 0.05 compared with WT alcohol by 1-way ANOVA). Av, autophagosomes; Avd, autolysosomes; AV, autophagic vacuoles. D: representative EM images are shown for the Gao-binge model with boxed areas enlarged (arrows represent autophagosomes, and arrowheads represent autolysosomes; bar = 500 nm). E and F: quantification of the number of autophagic vacuoles (E) and mitophagosomes (F) from EM in D. Data shown are means \pm SE (n = 1 mouse per group, at least 15 images quantified per mouse; * P < 0.05 compared with WT control, ** P < 0.05 compared with WT alcohol by 1-way ANOVA).



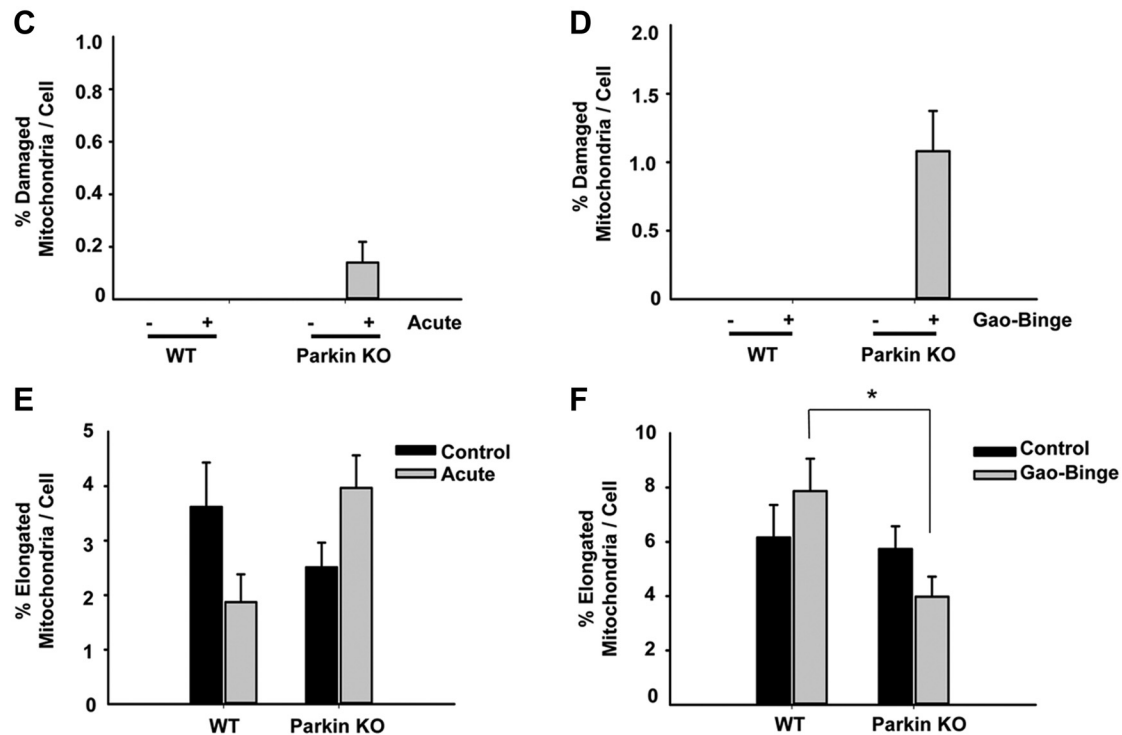


Fig. 6—Continued

after acute-binge treatment than WT mouse liver mitochondria. There were no significant differences in basal levels of COX activity between WT and Parkin KO mice (Fig. 7D). Interestingly, there were no significant differences in COX activity between control diet and Gao-binge-treated WT or Parkin KO mice (Fig. 7E). These data suggest that liver mitochondria in WT mice were likely adapting to alcohol treatment, and Parkin KO mouse mitochondria were unable to adapt as well as WT mice to alcohol treatment. Overall, these data suggest that Parkin KO mouse livers had more mitochondrial damage initiated by alcohol treatment than WT mouse livers, which likely led to their increased liver injury in the acute-binge and Gao-binge models and increased steatosis in the acute-binge model compared with WT mice.

Parkin KO mice had increased lipid peroxidation after alcohol administration. Alcohol is well known to cause oxidative stress and increased 4HNE staining as a result of increased lipid peroxidation in the liver (40). WT and Parkin KO mice had increased lipid peroxidation after both acute-binge and Gao-binge alcohol treatments, which was demonstrated by increased 4HNE staining (Fig. 8, A–D). We also found that 4HNE staining occurred mainly in the pericentral vein areas in both WT and Parkin KO mouse livers. In addition, Parkin KO mice had increased lipid peroxidation compared with WT mice after alcohol treatment in both the

acute-binge and Gao-binge models (Fig. 8, A–D). Control levels of lipid peroxidation were similar between WT and Parkin KO mice (Fig. 8, A–D). These results suggest that Parkin KO mice had higher levels of alcohol-induced oxidative stress compared with WT mice, which was likely due to the greater amount of alcohol-induced mitochondrial damage in Parkin KO mice compared with WT mice.

DISCUSSION

In this study, we found that Parkin KO mice had increased liver injury after alcohol treatment compared with WT mice with use of both the acute-binge and Gao-binge alcohol models. In addition, we found that Parkin KO mice had increased steatosis in the acute-binge model compared with WT mice, but levels of steatosis were similar between WT and Parkin KO mice after Gao-binge treatment. Increases in liver injury and steatosis in Parkin KO mice were likely due to an increase in alcohol-mediated mitochondrial damage and dysfunction in Parkin KO mouse livers compared with WT mouse livers because Parkin KO mouse livers had severely swollen and damaged mitochondria that lacked cristae after alcohol treatment, which were not observed in WT mouse livers. In addition, Parkin KO mouse livers had decreased mitophagy, β -oxidation, mitochondrial respiration, and COX activity compared

Fig. 6. Analysis of mitochondrial morphology after alcohol treatment in WT and Parkin KO mice. A and B: representative EM images are shown from WT and Parkin KO mice treated with the acute-binge (A) or Gao-binge (B) model with boxed areas enlarged. a: WT control. b: WT alcohol. c: Parkin KO control. d: Parkin KO alcohol. *Severely damaged mitochondria. Bar = 500 nm with the exception of Ad, which is 2 μ m. C and D: quantification of the number of severely damaged mitochondria shown in Ad and Bd in WT and Parkin KO mice after acute-binge (C) or Gao-binge (D) ($n \geq 10$ images per mouse from 2 mice per group). E and F: quantification of the number of elongated mitochondria per cell in WT and Parkin KO mice after acute-binge (E) or Gao-binge (F). Data shown are means \pm SE ($n \geq 10$ images per mouse from 2 mice per group; * $P < 0.05$ by 1-way ANOVA).

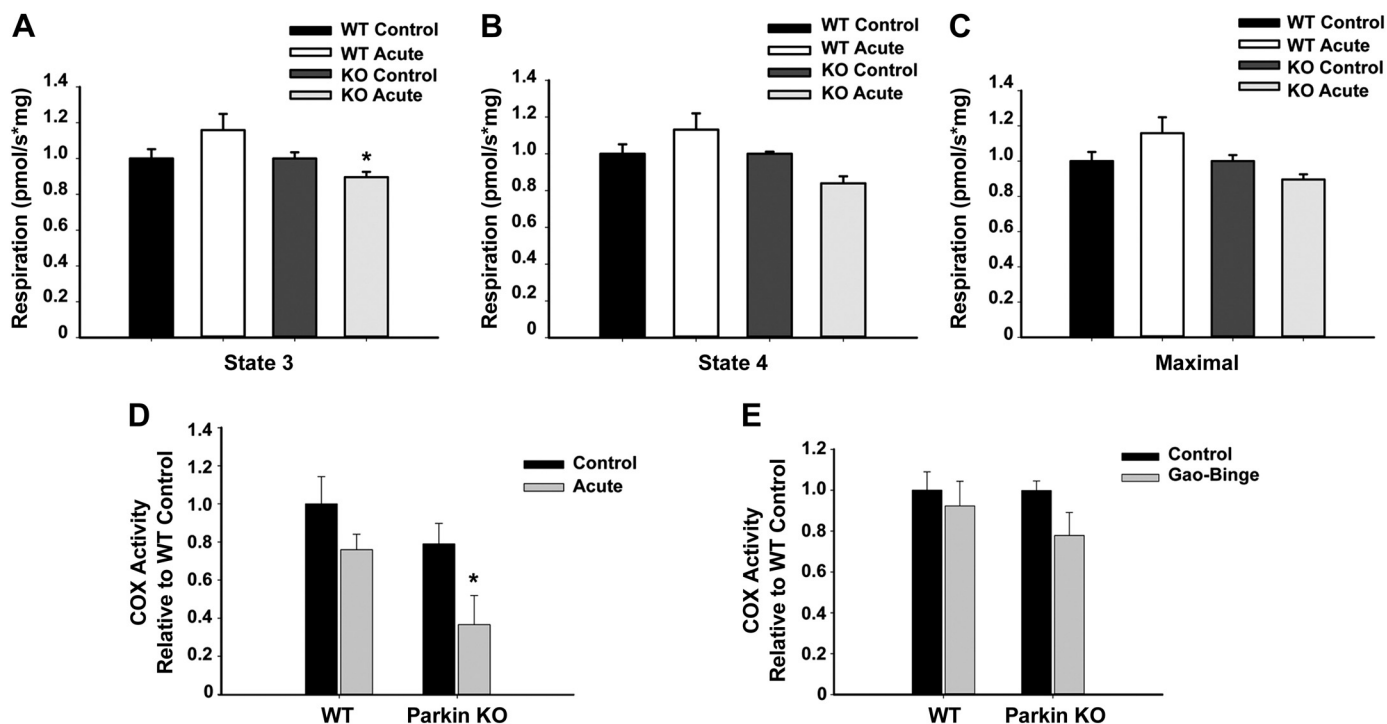


Fig. 7. Mitochondrial respiration rates and cytochrome *c* oxidase (COX) activity were decreased in Parkin KO mice after alcohol treatment. A–C: WT and Parkin KO mice were treated with alcohol by using the acute-binge model, and state 3 (A), state 4 (B), and maximal respiratory capacity (C) respiration rates were measured by Oroboros using isolated liver mitochondria. Data shown are means \pm SE ($n \geq 3$ mice per group; * $P < 0.05$ compared with WT alcohol by *t*-test). D and E: COX activity for WT and Parkin KO mouse livers treated with acute-binge (D) or Gao-binge (E). Data shown are means \pm SE ($n \geq 3$ mice per group; * $P < 0.05$ compared with WT control by 1-way ANOVA).

with WT mouse livers after acute-binge alcohol treatment. Decreases in Parkin KO mouse mitochondrial function were likely due to increased alcohol-induced mitochondrial damage and reduced mitophagy in Parkin KO mouse livers compared with WT mouse livers. In addition, mitochondria from Parkin KO mouse livers seemed less able to adapt to alcohol compared with WT mouse mitochondria, resulting in severely damaged and swollen mitochondria in Parkin KO mouse livers. Furthermore, Parkin KO mouse livers had greater alcohol-induced oxidative stress-mediated lipid peroxidation compared with WT mouse livers. Therefore, our findings suggest that Parkin is an important protector against alcohol-induced liver injury and steatosis by maintaining mitochondrial integrity and function likely via mitophagy induction after alcohol treatment.

Parkin-mediated mitophagy likely protects against alcohol-induced liver injury. Mitophagy is a well-known protective mechanism for removing damaged mitochondria to prevent cell death and liver injury. For example, mitophagy has been shown to be protective against apoptosis and injury in alcoholic liver disease (9, 21) and also against necrosis in acetaminophen-induced liver injury (22, 30, 32, 38). However, the mechanism for how mitophagy is induced in the liver by alcohol is currently unknown. Parkin translocated to mitochondria after Gao-binge alcohol treatment in WT mice, suggesting that Parkin-induced mitophagy did occur after alcohol treatment. EM analysis showed that mitophagosome numbers were significantly increased in WT mouse livers, but not in Parkin KO mouse livers, after acute-binge and Gao-binge alcohol treatment compared with controls. These results suggest a

possible defect in mitophagy induction after alcohol treatment in Parkin KO mice. Unfortunately, there is currently no reliable quantitative assay to quantify mitophagy *in vivo*, particularly in the liver. We could not detect any differences in LC3-II, p62, or mitochondria protein levels between WT and Parkin KO mice before or after alcohol treatment by Western blot analysis. This could be due to at least two reasons. First, alcohol-induced mitophagy could be mild in the mouse livers compared with other mitophagy models such as acetaminophen-induced mitophagy. Second, liver cells may adapt to alcohol-induced mitochondrial damage by activating mitochondrial biogenesis, which may offset the autophagic degradation of mitochondrial proteins as assessed by Western blot analysis.

It should be noted that alcohol could still induce mitophagy in Parkin KO mouse livers as assessed by EM studies, although the number of mitophagosomes was significantly decreased compared with WT mice. These results suggest that other compensatory mechanisms may exist for mitophagy induction in the liver in the absence of Parkin. There are several other proteins that have been shown to have important roles in the mitophagy pathway that may help compensate for loss of Parkin in the liver. For example, there are other E3 ligases such as Smurf1 and Mul1 that have been shown to have a role in mitophagy induction. In addition, Bnip3, Fundc1, and Nix have been shown to have roles in mitophagy induction during hypoxia, and the inner mitochondrial phospholipid cardiolipin has also recently been shown to be able to induce mitophagy in neurons (31). Therefore, it is possible that one or several of these proteins are upregulated in the absence of Parkin to

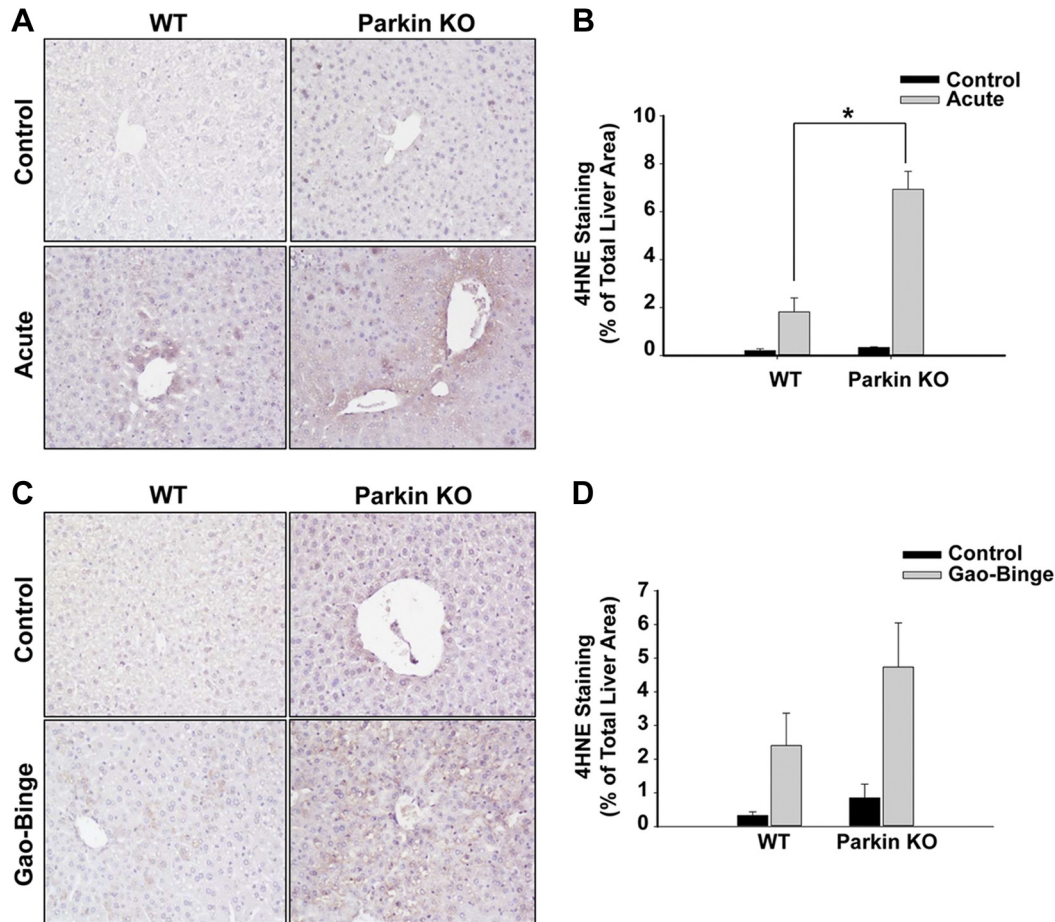


Fig. 8. Lipid peroxidation was increased in Parkin KO mice compared with WT mice after alcohol treatment. A–D: WT and Parkin KO mice were treated with alcohol by using the acute-binge (A and B) or Gao-binge (C and D) model. Representative images are shown from 4-hydroxynonenal (4HNE) immunohistochemistry after acute-binge (A) or Gao-binge (C) treatment, and data are represented as the percent (%) of positively stained areas compared with the total liver area [B (acute), D (Gao-Binge)]. Results shown are means \pm SE ($n \geq 3$ mice per group; * $P < 0.05$ compared with WT control by 1-way ANOVA).

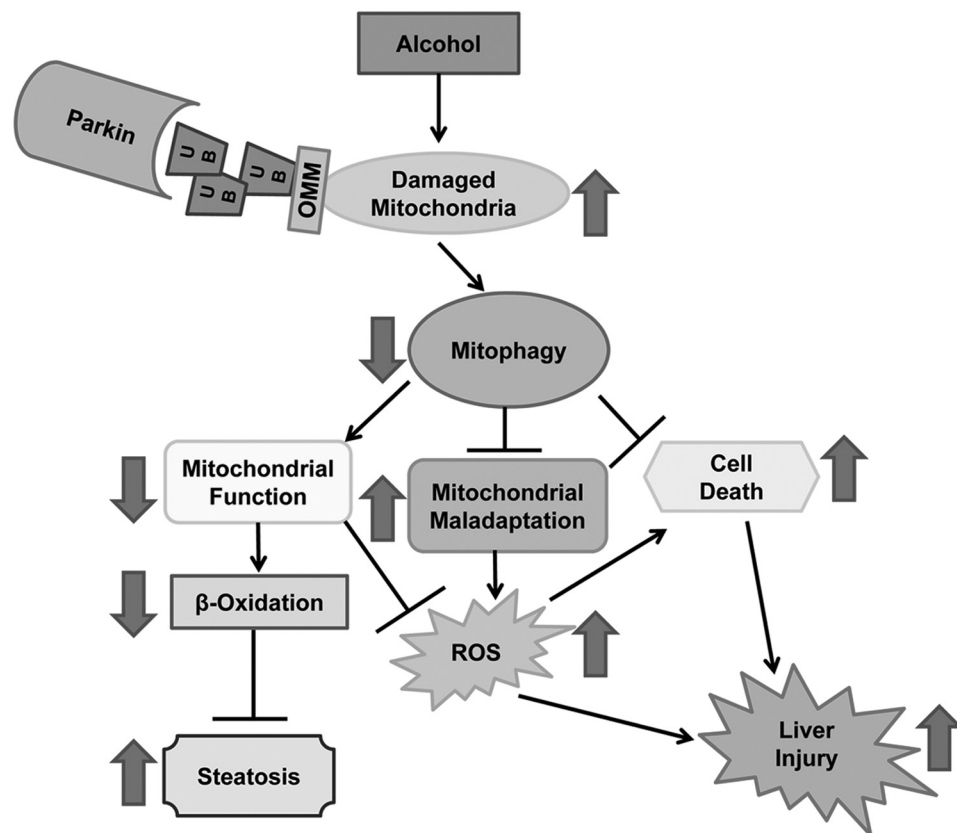
induce Parkin-independent mitophagy in the liver. However, the exact mediator of Parkin-independent mitophagy induction in the liver still needs further investigation.

Overall, Parkin-induced mitophagy was likely a protective mechanism in the liver after alcohol treatment because Parkin KO mice had reduced mitophagy levels and increased liver injury after alcohol administration compared with WT mice. However, we have only shown an associative relationship between reduced mitophagy and alcohol-induced liver injury in Parkin KO mice. Therefore, it is also possible that Parkin plays other roles in maintaining mitochondrial function in addition to mitophagy that may protect against alcohol-induced liver injury.

Acute-binge and Gao-binge alcohol treatments had differential effects on β -oxidation. We found that both the acute-binge and Gao-binge models caused hepatic steatosis, and increased steatosis was likely not due to increased fatty acid synthesis. Lee and colleagues (47) also showed that acute-binge treatment for 24 h did not result in increased fatty acid synthesis. The effect of the Gao-binge model on fatty acid synthesis has not been previously investigated. Interestingly, we observed that only the acute-binge model, but not the Gao-binge model, caused greater steatosis in the livers of Parkin KO mice compared with WT mice. These observations are associated with different effects of the two alcohol models

on β -oxidation. In the acute-binge model, several β -oxidation genes were induced in WT mouse livers after alcohol treatment but were left unchanged in Parkin KO mouse livers, suggesting that Parkin KO mouse mitochondria lacked the ability to induce β -oxidation as a protective mechanism. This inability to induce β -oxidation after acute-binge treatment likely led to their increased levels of liver steatosis compared with WT mice. Gao-binge treatment did not cause induction of β -oxidation genes in either WT or Parkin KO mouse livers, suggesting that β -oxidation was inhibited in both WT and Parkin KO mouse livers after Gao-binge alcohol treatment. This may help to explain why the levels of steatosis were similar between WT and Parkin KO mice after Gao-binge alcohol treatment. Chronic alcohol feeding is well known to cause inhibition of β -oxidation, leading to accumulation of fat in the liver (24). It seems that liver cells were able to adapt to alcohol-induced injury by increasing β -oxidation in acute-binge-treated WT but not in Parkin KO mouse livers. However, this adaptation seemed to be lost after Gao-binge treatment. In addition to β -oxidation, the acute-binge and Gao-binge alcohol models may also dissimilarly affect fat uptake or secretion, which could lead to differences in levels of liver steatosis after alcohol treatment between these models. Differences in alco-

Fig. 9. Summary of the role of Parkin in alcohol-induced steatosis and liver injury. Parkin is protective against alcohol-induced liver injury, oxidative stress, and steatosis by promoting mitophagy. Decreased mitophagy due to the absence of Parkin may lead to impaired mitochondrial function, decreased β oxidation, increased reactive oxygen species, and lipid peroxidation as well as mitochondrial maladaptation (fewer elongated mitochondria and more swollen mitochondria), resulting in increased steatosis, cell death, and liver injury after alcohol treatment. Consequences of Parkin loss after alcohol treatment are shown by large arrows. ROS, reactive oxygen species; UB, ubiquitin; OMM, outer mitochondrial membrane protein.



hol-induced fat uptake and secretion between the acute-binge and Gao-binge models remain to be investigated.

Parkin KO mice had increased numbers of severely damaged liver mitochondria and were less able to adapt to alcohol treatment, leading to decreased mitochondrial function, increased oxidative stress, and increased liver injury and steatosis. After acute-binge and Gao-binge alcohol treatments, *Parkin KO* mouse livers had severely damaged and swollen mitochondria that lacked cristae, which were not seen in WT mouse livers. In addition, after Gao-binge treatment, WT mouse livers had more elongated mitochondria, which is thought to be a cellular adaptive mechanism to chronic alcohol treatment (15), than *Parkin KO* mouse livers. Furthermore, after alcohol treatment *Parkin KO* mouse livers had greater levels of lipid peroxidation than WT mouse livers, which was likely caused by oxidative stress mediated by alcohol-induced mitochondrial damage. These results all suggest that mitochondria in *Parkin KO* mouse livers were more damaged and dysfunctional compared with WT liver mitochondria after alcohol treatment.

Indeed, we found that WT mouse liver mitochondria had increased Complex I respiration rates whereas *Parkin KO* mouse liver mitochondria had decreased respiration rates after acute-binge alcohol treatment compared with controls. It has been shown that WT mice have increased respiration rates after oral alcohol feeding and intragastric infusion of alcohol, which was thought to be due to increased incorporation of respiratory complexes into the electron transport chain as an adaptation method (15). However, Bailey and colleagues (18) showed that state 3 respiration was unaffected by chronic alcohol feeding whereas state 4 respiration was increased. Differences in their

results were likely due to the alcohol models or alcohol doses used. We observed increased respiration in WT mice treated with acute-binge for both state 3 and state 4 respiration, although it did not reach statistical significance. However, we found significantly decreased respiration in *Parkin KO* mice for state 3 respiration after acute-binge. Moreover, *Parkin KO* mice had decreased COX activity after acute-binge alcohol treatment compared with WT mice. These results suggest that *Parkin KO* mouse liver mitochondria either were more damaged by alcohol treatment or lacked the ability to adapt to alcohol treatment compared with WT mice. WT, but not *Parkin KO*, mouse mitochondria were likely attempting to adapt to alcohol treatment by increasing their respiration rates. It was previously shown that *Parkin KO* mice had decreased basal brain mitochondria respiration rates at 8 mo of age compared with WT mice (33). We did not see any differences in basal liver respiration rates between WT and *Parkin KO* mouse livers at 2–3 mo of age. It would be interesting to investigate whether respiration rates are overall decreased in aged *Parkin KO* mouse livers and whether this would have an impact on their alcohol-induced liver injury in the future.

Mitochondria are dynamic organelles that are well known to alter their fission and fusion rates to adapt to stress to maintain cellular survival. These fission and fusion events are necessary for cell survival because they allow the cell to adapt to changing conditions needed for cell growth, division, and distribution of mitochondria (43). Mitochondria elongation was seen in chronic alcohol feeding and was suggested to be an adaptive response to alcohol treatment (15). WT mouse livers had many elongated mitochondria after Gao-binge treatment, but *Parkin KO* mouse livers had less elongated and more

swollen mitochondria than WT mouse livers. Parkin has been shown to play a role in regulating mitochondrial fusion and fission by promoting proteasomal degradation of mitofusin 1 and mitofusin 2 as well as Drp1 (8, 44). Future work is needed to determine whether these mitochondrial fusion and fission machinery proteins play a role in the elongated mitochondria observed in WT mouse livers exposed to alcohol. Nevertheless, these observations regarding mitochondrial morphology together with the mitochondrial respiration and COX activity data further support the notion that WT liver mitochondria seemed more able to adapt to alcohol treatment than Parkin KO mouse liver mitochondria. Overall, these data suggest that alcohol caused more damage to mitochondria in Parkin KO mouse livers than in WT mouse livers, which likely led to the increased liver injury and steatosis seen in Parkin KO mice compared with WT mice.

Concluding remarks. In conclusion, we found that alcohol caused more liver injury, oxidative stress, and steatosis in Parkin KO mice compared with WT mice, likely due to increased mitochondrial damage and dysfunction in Parkin KO mouse livers compared with WT mouse livers after alcohol treatment. This increase in mitochondrial damage and dysfunction in Parkin KO mice may have been partly due to decreased mitophagy in these mice. However, it is likely that Parkin may have other roles in maintaining mitochondrial function, such as regulation of mitochondrial dynamics in addition to mitophagy, that are also important for protection against alcohol-induced steatosis and liver injury. The possible molecular events involved in Parkin-mediated mitophagy and mitochondrial functions for regulating alcohol-induced steatosis and liver injury are summarized in Fig. 9.

ACKNOWLEDGMENTS

The authors thank Barbara Fegley from the electron microscopy core facility at the University of Kansas Medical Center for excellent assistance for EM studies. The authors also thank Dr. Russell Swerdlow and Dr. Heather Wilkins for assistance with Oroboros experiments, Long Wu for help with optimizing the COX activity assay, and Shaogui Wang and Yuan Li for help with animal experiments.

GRANTS

The research was supported in part by the National Institute on Alcohol Abuse and Alcoholism funds R01 AA020518, R01 DK102142, National Center for Research Resources (5P20RR021940), the National Institute of General Medical Sciences (8P20 GM103549), T32 ES007079, an Institutional Development Award (IDeA) from the National Institute of General Medical Sciences of the National Institutes of Health (P20 GM103418), and an award received in an internal Lied basic science grant program of the University of Kansas Medical Center Research Institute, with support from a NIH Clinical and Translational Science Award grant (UL1TR000001, formerly UL1RR033179). The electron microscopy core facility is supported in part, by NIH COBRE grant 9P20GM104936. The JEOL JEM-1400 TEM used in the study was purchased with funds from NIH grant S10RR027564.

DISCLOSURES

No conflicts of interest, financial or otherwise, are declared by the author(s).

AUTHOR CONTRIBUTIONS

J.A.W. and H.-M.N. performed experiments; J.A.W., Y.D., and W.-X.D. analyzed data; J.A.W. and W.-X.D. interpreted results of experiments; J.A.W. prepared figures; J.A.W. drafted manuscript; J.A.W. and W.-X.D. edited and revised manuscript; J.A.W., H.-M.N., Y.D., and W.-X.D. approved final version of manuscript; W.-X.D. conception and design of research.

REFERENCES

- Andringa KK, Udoh US, Landar A, Bailey SM. Proteomic analysis of 4-hydroxynonenal (4-HNE) modified proteins in liver mitochondria from chronic ethanol-fed rats. *Redox Biol* 2C: 1038–1047, 2014.
- Bansal S, Liu CP, Sepuri NB, Anandatheerthavarada HK, Selvaraj V, Hoek J, Milne GL, Guengerich FP, Avadhani NG. Mitochondria-targeted cytochrome P450 2E1 induces oxidative damage and augments alcohol-mediated oxidative stress. *J Biol Chem* 285: 24609–24619, 2010.
- Bertola A, Mathews S, Ki SH, Wang H, Gao B. Mouse model of chronic and binge ethanol feeding (the NIAAA model). *Nat Protoc* 8: 627–637, 2013.
- Bertola A, Park O, Gao B. Chronic plus binge ethanol feeding synergistically induces neutrophil infiltration and liver injury in mice: a critical role for E-selectin. *Hepatology* 58: 1814–1823, 2013.
- Bruha R, Dvorak K, Petrtyl J. Alcoholic liver disease. *World J Hepatol* 4: 81–90, 2012.
- Chan NC, Chan DC. Parkin uses the UPS to ship off dysfunctional mitochondria. *Autophagy* 7: 771–772, 2011.
- Chan NC, Salazar AM, Pham AH, Sweredoski MJ, Kolawa NJ, Graham RL, Hess S, Chan DC. Broad activation of the ubiquitin-proteasome system by Parkin is critical for mitophagy. *Hum Mol Genet* 20: 1726–1737, 2011.
- Ding WX, Guo F, Ni HM, Bockus A, Manley S, Stolz DB, Eskelinen EL, Jaeschke H, Yin XM. Parkin and mitofusins reciprocally regulate mitophagy and mitochondrial spheroid formation. *J Biol Chem* 287: 42379–42388, 2012.
- Ding WX, Li M, Chen X, Ni HM, Lin CW, Gao W, Lu B, Stolz DB, Clemens DL, Yin XM. Autophagy reduces acute ethanol-induced hepatotoxicity and steatosis in mice. *Gastroenterology* 139: 1740–1752, 2010.
- Ding WX, Li M, Yin XM. Selective taste of ethanol-induced autophagy for mitochondria and lipid droplets. *Autophagy* 7: 248–249, 2011.
- Ding WX, Ni HM, DiFrancesca D, Stolz DB, Yin XM. Bid-dependent generation of oxygen radicals promotes death receptor activation-induced apoptosis in murine hepatocytes. *Hepatology* 40: 403–413, 2004.
- Ding WX, Yin XM. Mitophagy: mechanisms, pathophysiological roles, analysis. *Biol Chem* 393: 547–564, 2012.
- Gao B, Bataller R. Alcoholic liver disease: pathogenesis and new therapeutic targets. *Gastroenterology* 141: 1572–1585, 2011.
- Garcia-Ruiz C, Kaplowitz N, Fernandez-Checa JC. Role of mitochondria in alcoholic liver disease. *Curr Pathobiol Rep* 1: 159–168, 2013.
- Han D, Ybanez MD, Johnson HS, McDonald JN, Mesrobian L, Sancheti H, Martin G, Martin A, Lim AM, Dara L, Cadenas E, Tsukamoto H, Kaplowitz N. Dynamic adaptation of liver mitochondria to chronic alcohol feeding in mice: biogenesis, remodeling, and functional alterations. *J Biol Chem* 287: 42165–42179, 2012.
- Ji C, Chan C, Kaplowitz N. Predominant role of sterol response element binding proteins (SREBP) lipogenic pathways in hepatic steatosis in the murine intragastric ethanol feeding model. *J Hepatol* 45: 717–724, 2006.
- Kawajiri S, Saiki S, Sato S, Sato F, Hatano T, Eguchi H, Hattori N. PINK1 is recruited to mitochondria with parkin and associates with LC3 in mitophagy. *FEBS Lett* 584: 1073–1079, 2010.
- King AL, Swain TM, Mao Z, Udoh US, Oliva CR, Betancourt AM, Griguer CE, Crowe DR, Lesort M, Bailey SM. Involvement of the mitochondrial permeability transition pore in chronic ethanol-mediated liver injury in mice. *Am J Physiol Gastrointest Liver Physiol* 306: G265–G277, 2014.
- Kitada T, Asakawa S, Hattori N, Matsumine H, Yamamura Y, Minoshima S, Yokochi M, Mizuno Y, Shimizu N. Mutations in the parkin gene cause autosomal recessive juvenile parkinsonism. *Nature* 392: 605–608, 1998.
- Leung TM, Nieto N. CYP2E1 and oxidant stress in alcoholic and non-alcoholic fatty liver disease. *J Hepatol* 58: 395–398, 2013.
- Lin CW, Zhang H, Li M, Xiong X, Chen X, Chen X, Dong XC, Yin XM. Pharmacological promotion of autophagy alleviates steatosis and injury in alcoholic and non-alcoholic fatty liver conditions in mice. *J Hepatol* 58: 993–999, 2013.
- Lin Z, Wu F, Lin S, Pan X, Jin L, Lu T, Shi L, Wang Y, Xu A, Li X. Adiponectin protects against acetaminophen-induced mitochondrial dysfunction and acute liver injury by promoting autophagy in mice. *J Hepatol* 61: 825–831, 2014.
- Liu L, Sakakibara K, Chen Q, Okamoto K. Receptor-mediated mitophagy in yeast and mammalian systems. *Cell Res* 24: 787–795, 2014.

24. Mantena SK, King AL, Andringa KK, Eccleston HB, Bailey SM. Mitochondrial dysfunction and oxidative stress in the pathogenesis of alcohol- and obesity-induced fatty liver diseases. *Free Radic Biol Med* 44: 1259–1272, 2008.
25. Mathews S, Xu M, Wang H, Bertola A, Gao B. Animals models of gastrointestinal and liver diseases. Animal models of alcohol-induced liver disease: pathophysiology, translational relevance, and challenges. *Am J Physiol Gastrointest Liver Physiol* 306: G819–G823, 2014.
26. Matsuda N, Sato S, Shiba K, Okatsu K, Saisho K, Gautier CA, Sou YS, Saiki S, Kawajiri S, Sato F, Kimura M, Komatsu M, Hattori N, Tanaka K. PINK1 stabilized by mitochondrial depolarization recruits Parkin to damaged mitochondria and activates latent Parkin for mitophagy. *J Cell Biol* 189: 211–221, 2010.
27. Narendra D, Tanaka A, Suen DF, Youle RJ. Parkin is recruited selectively to impaired mitochondria and promotes their autophagy. *J Cell Biol* 183: 795–803, 2008.
28. Nassir F, Ibdah JA. Role of mitochondria in alcoholic liver disease. *World J Gastroenterol* 20: 2136–2142, 2014.
29. Ni HM, Bhakta A, Wang S, Li Z, Manley S, Huang H, Copple B, Ding WX. Role of hypoxia inducing factor-1beta in alcohol-induced autophagy, steatosis and liver injury in mice. *PLoS One* 9: e115849, 2014.
30. Ni HM, Bockus A, Boggess N, Jaeschke H, Ding WX. Activation of autophagy protects against acetaminophen-induced hepatotoxicity. *Hepatology* 55: 222–232, 2012.
31. Ni HM, Williams JA, Ding WX. Mitochondrial dynamics and mitochondrial quality control. *Redox Biol* 4C: 6–13, 2015.
32. Ni HM, Williams JA, Jaeschke H, Ding WX. Zonated induction of autophagy and mitochondrial spheroids limits acetaminophen-induced necrosis in the liver. *Redox Biol* 1: 427–432, 2013.
33. Palacino JJ, Sagi D, Goldberg MS, Krauss S, Motz C, Wacker M, Klose J, Shen J. Mitochondrial dysfunction and oxidative damage in parkin-deficient mice. *J Biol Chem* 279: 18614–18622, 2004.
34. Parzych KR, Klionsky DJ. An overview of autophagy: morphology, mechanism, and regulation. *Antioxid Redox Signal* 20: 460–473, 2014.
35. Periquet M, Corti O, Jacquier S, Brice A. Proteomic analysis of parkin knockout mice: alterations in energy metabolism, protein handling and synaptic function. *J Neurochem* 95: 1259–1276, 2005.
36. Rehman J, Samokhvalov AV, Shield KD. Global burden of alcoholic liver diseases. *J Hepatol* 59: 160–168, 2013.
37. Robin MA, Sauvage I, Grandperret T, Descatoire V, Pessayre D, Fromenty B. Ethanol increases mitochondrial cytochrome P450 2E1 in mouse liver and rat hepatocytes. *FEBS Lett* 579: 6895–6902, 2005.
38. Saberi B, Ybanez MD, Johnson HS, Gaarde WA, Han D, Kaplowitz N. Protein kinase C (PKC) participates in acetaminophen hepatotoxicity through c-jun-N-terminal kinase (JNK)-dependent and -independent signaling pathways. *Hepatology* 59: 1543–1554, 2014.
39. Shukla SD, Pruett SB, Szabo G, Arteel GE. Binge ethanol and liver: new molecular developments. *Alcohol Clin Exp Res* 37: 550–557, 2013.
40. Smathers RL, Galligan JJ, Stewart BJ, Petersen DR. Overview of lipid peroxidation products and hepatic protein modification in alcoholic liver disease. *Chem Biol Interact* 192: 107–112, 2011.
41. Sozio M, Crabb DW. Alcohol and lipid metabolism. *Am J Physiol Endocrinol Metab* 295: E10–E16, 2008.
42. Stichel CC, Zhu XR, Bader V, Linnartz B, Schmidt S, Lubbert H. Mono- and double-mutant mouse models of Parkinson's disease display severe mitochondrial damage. *Hum Mol Genet* 16: 2377–2393, 2007.
43. van der Blik AM, Shen Q, Kawajiri S. Mechanisms of mitochondrial fission and fusion. *Cold Spring Harb Perspect Biol* 5: a011072, 2013.
44. Wang H, Song P, Du L, Tian W, Yue W, Liu M, Li D, Wang B, Zhu Y, Cao C, Zhou J, Chen Q. Parkin ubiquitinates Drp1 for proteasome-dependent degradation: implication of dysregulated mitochondrial dynamics in Parkinson disease. *J Biol Chem* 286: 11649–11658, 2011.
45. Williams JA, Manley S, Ding WX. New advances in molecular mechanisms and emerging therapeutic targets in alcoholic liver diseases. *World J Gastroenterol* 20: 12908–12933, 2014.
46. Williams JA, Ni HM, Haynes A, Manley S, Li Y, Jaeschke H, Ding WX. Chronic deletion and acute knockdown of parkin have differential responses to acetaminophen-induced mitophagy and liver injury in mice. *J Biol Chem* 290: 10934–10946, 2015.
47. Yin HQ, Kim M, Kim JH, Kong G, Kang KS, Kim HL, Yoon BI, Lee MO, Lee BH. Differential gene expression and lipid metabolism in fatty liver induced by acute ethanol treatment in mice. *Toxicol Appl Pharmacol* 223: 225–233, 2007.
48. You M, Fischer M, Deeg MA, Crabb DW. Ethanol induces fatty acid synthesis pathways by activation of sterol regulatory element-binding protein (SREBP). *J Biol Chem* 277: 29342–29347, 2002.
49. Zelickson BR, Benavides GA, Johnson MS, Chacko BK, Venkatraman A, Landar A, Betancourt AM, Bailey SM, Darley-Usmar VM. Nitric oxide and hypoxia exacerbate alcohol-induced mitochondrial dysfunction in hepatocytes. *Biochim Biophys Acta* 1807: 1573–1582, 2011.